

# THE EFFECT OF PRESSURE ON HEAT TRANSFER DURING POOL BOILING OF WATER- $\text{Al}_2\text{O}_3$ AND WATER-CU NANOFLUIDS ON STAINLESS STEEL SMOOTH TUBE

Janusz T. Cieśliński\*, Tomasz Z. Kaczmarczyk

Gdansk University of Technology, Narutowicza 11/12, 80-233 Gdańsk, Poland

Experimental investigation of heat transfer during pool boiling of two nanofluids, i.e. water- $\text{Al}_2\text{O}_3$  and water-Cu has been carried out. Nanoparticles were tested at the concentration of 0.01%, 0.1%, and 1% by weight. The horizontal smooth stainless steel tubes having 10 mm OD and 0.6 mm wall thickness formed the test heater. The experiments have been performed to establish the influence of nanofluids concentration on heat transfer characteristics during boiling at different absolute operating pressure values, i.e. 200 kPa, ca. 100 kPa (atmospheric pressure) and 10 kPa. It was established that independent of nanoparticle materials ( $\text{Al}_2\text{O}_3$  and Cu) and their concentration, an increase of operating pressure enhances heat transfer. Generally, independent of operating pressure, sub- and atmospheric pressure, and overpressure, an increase of nanoparticle concentration caused heat transfer augmentation.

**Keywords:** pool boiling, nanofluids, operating pressure

## 1. INTRODUCTION

Necessity of energy saving, miniaturization of heat exchangers and ultra-high heat duty devices stimulate application of new heat transfer technologies. One possibility to solve the problem is to apply enhanced surfaces (Bergles, 1985). Another possibility results from modification of thermal properties of fluids. As a result of recent advances in nanoscale science new category of fluids termed nanofluids has been developed. Nanofluid is a suspension which consists of the base liquid and metallic or non-metallic nanoparticles with a typical size less than 100 nm (Choi, 1995). The promise of nanofluids arises from the fact that relatively small concentration of nanoparticles, typically below 5% by volume, significantly enhances thermal conductivity of the fluid (Kleinstreuer, 2011). Though the augmentation of thermal conductivity of slurries is a well known fact, they have not been used due to problems associated with them such as sedimentation, erosion and fouling. Because of extremely small size of nanoparticles, problems with clogging, fouling or even damage of flow loop devices can be avoided while providing the cooling benefit.

Nanofluids have been considered as the working fluid for thermosyphons (Cieśliński and Rubalewski, 2012; Yang and Liu, 2011) and heat pipes in electronic cooling applications (Kang et al., 2006). The addition of nanoparticles to the standard engine coolant has the potential to improve automotive and heavy-duty engine cooling rates (Leong et al., 2010). Bi et al., 2011 reported that nanorefrigerant application in a domestic refrigerator resulted in energy consumption reduction as well as in freezing velocity increase. The development of stable nanofluids for use in water-cooled nuclear systems could

\*Corresponding author, e-mail: jcieslin@pg.gda.pl

result in a significant improvement of their economic performance and/or safety margins (Hadad et al., 2010; Kim et al., 2010).

As regards pool boiling, some studies report no change of heat transfer in the nucleate boiling regime (Kwark et al., 2010; Vassallo et al., 2004), some report heat transfer deterioration (Bang and Chang, 2005; Lotfi and Shafii, 2009) and others heat transfer enhancement (Kathiravan et al., 2010; Li et al., 2003; Shi et al., 2006; Wen and Ding, 2005).

Many aspects of pool boiling of nanofluids were investigated, among others the effect of concentration of nanoparticles (Das et al., 2003; Trisaksri and Wongwises, 2009), the effect of nanoparticle material (Cieśliński and Kaczmarczyk, 2011; Lotfi and Shafii, 2009, Shi et al., 2006), the effect of heating surface orientation (Narayan et al., 2008), material and finish (Cieśliński and Kaczmarczyk, 2011; Coursey and Kim, 2008), the effect of base liquid (Liu and Liao, 2008). Only a few publications are devoted to the effect of pressure on pool boiling heat transfer of nanofluids.

Trisaksri and Wongwises (2009) tested R141b-TiO<sub>2</sub> nanofluid while boiling it on a horizontal copper cylinder of 28.5 mm in diameter. The measurements were performed within the range of 200-500 kPa and 0.01% - 0.05% of nanoparticle volume concentration. The heat transfer coefficient was found to increase with operating pressure increase. However at a very low heat flux, there is almost no effect of pressure on heat transfer coefficient. Additionally, for 0.05% nanoparticle concentration the influence of pressure on boiling heat transfer diminishes, especially at a higher pressure.

You et al. (2003) studied pool boiling of water-Al<sub>2</sub>O<sub>3</sub> nanofluid on polished copper (10x10 mm) surface at the pressure of 20.89 kPa. Tested concentrations of nanoparticles ranged from 0 g/l to 0.05 g/l. No appreciable differences in the boiling heat transfer were found for the heat flux less than the CHF.

Kashinath (2006) carried out experiments with pool boiling of water-Al<sub>2</sub>O<sub>3</sub> nanofluid on a copper block of 1x1 cm having 0.3 cm thickness under three operating pressures: 47.39 kPa, 19.94 kPa, and 7.38 kPa. The mass concentration of the nanoparticles was 0.025 g/l. Independent of operating pressure boiling curves for pure water and nanofluid coincided and heat transfer coefficient was found to increase with an increase in pressure.

Liu et al. (2007) performed experiments with boiling of water-Cu nanofluid on micro-grooved horizontal surface under four steady operating pressures of 100 kPa, 31.2 kPa, 20.0 kPa and 7.4 kPa. Nanoparticle concentration was 0.1%, 0.2%, 0.5%, 1%, and 1% by weight. The dimension of the face surface of the copper bar used as the heating surface was 40x40 mm. The tests indicated that the pressure has a very significant influence on heat transfer coefficient. Contrary to water boiling on smooth surface heat transfer coefficient for boiling of nanofluids greatly increases with a decrease of the test pressure.

Liu et al. (2010) investigated boiling of water-CNT suspensions on smooth copper surface. The mass concentration of the CNT (carbon nanotubes) was in the range of 0.5% to 4% by weight. The test runs were performed under three steady operating pressures of 103 kPa, 20.0 kPa and 7.4 kPa. The heat transfer coefficient increased with a decrease of operating pressure. The heat transfer coefficient can increase by a maximum of 60% at the atmospheric pressure, while by 130% at the pressure of 7.4 kPa.

Literature findings regarding influence of pressure lower than atmospheric on heat transfer during pool boiling of nanofluids can be summarized as follows: some studies report no change of heat transfer, some report heat transfer deterioration and others heat transfer enhancement.

As a consequence, the main aim of the present study was to obtain boiling characteristics, i.e. boiling curves and heat transfer coefficients for water-Al<sub>2</sub>O<sub>3</sub> and water-Cu nanofluids of different nanoparticle concentrations while boiling on horizontal, smooth stainless steel tube under different absolute

operating pressure, i.e. 200 kPa, ca. 100 kPa (atmospheric pressure) and 10 kPa. Nanoparticles were tested at the concentration of 0.01%, 0.1%, and 1% by weight. The horizontal smooth - finished with emery paper 360 ( $R_a=0.06 \mu\text{m}$ ), stainless steel tube having 10 mm OD and 0.6 mm wall thickness formed the test heater.

## 2. EXPERIMENTAL

### 2.1. Experimental set up

Figure 1 shows a schematic diagram of the experimental apparatus. The test chamber consisted of a cubical vessel made of stainless steel with inside dimensions of 150 mm x 150 mm x 250 mm. The horizontal stainless steel tube having 10 mm OD and 0.6 mm wall thickness formed the test heater. The effective length of the test tube was 100 mm. The tube was roughed with emery paper 360, so  $R_a=0.06 \mu\text{m}$ . A resistance cartridge heater was inserted into the test tube to generate heat flux from an electrical power supply. The power supply can be adjusted by an electrical transformer. Great care must be exercised with the cartridge heater and temperature measuring instrumentation to ensure good accuracy of measurements of the inside temperature of the heating cylinder (Marto and Anderson, 1992). The final design of the present heating section has been established after many practical trials supported by numerical simulations of 3D temperature fields (Cieśliński et al., 2007). Twelve K-type thermocouples installed in the grooves of a copper sleeve placed inside the tube were used to measure inside temperature of the tube. The detailed geometry of the test tube is shown in Fig. 2. The liquid level was maintained at ca. 15 mm above the centerline of the test tube. In a typical experiment, before the test began, a vacuum pump was used to evacuate the accumulated air from the vessel. Nanofluid at a pre-set concentration was charged and then preheated to the saturated temperature by an auxiliary heater. Next, the cartridge heater was switched on. Measurements were first performed at the lowest power input. Data were collected by increasing the heat flux by small increments. Experiments were performed for three values of absolute pressure in the test chamber, i.e. 200 kPa, ca. 100 kPa (atmospheric pressure) and 10 kPa. In order to ensure consistent surface state after each test the boiling surface was prepared in the same manner, i.e. the stainless steel tube was roughed with emery paper 360 and next the test tube was placed in an ultrasonic cleaner for 1 h. Finally, the boiling surface was cleaned by a water jet.

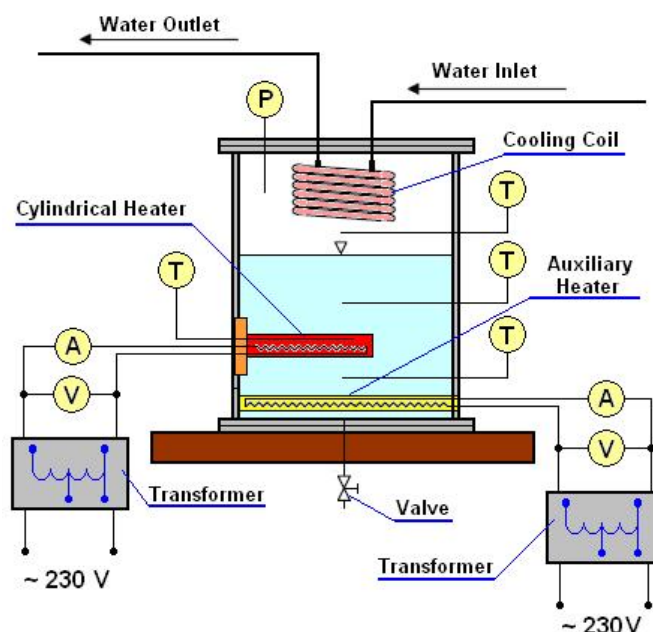


Fig. 1. Scheme of the experimental rig

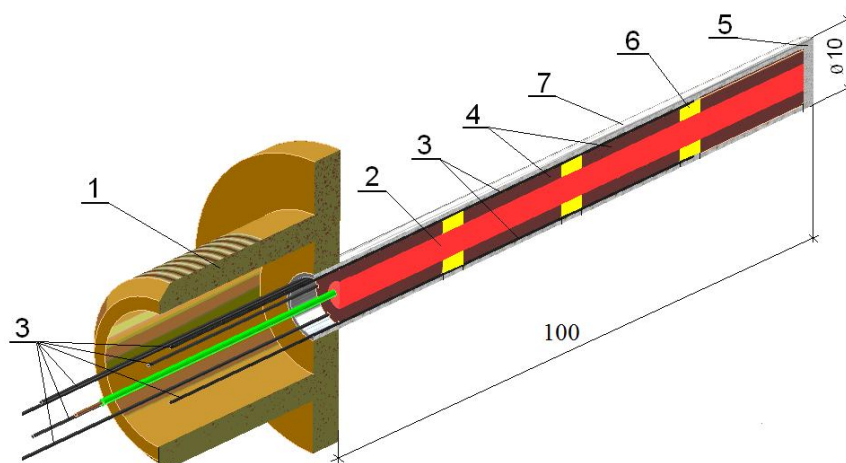


Fig. 2. Details of the test section,  
1 – flange, 2 – cartridge heater, 3 – thermocouples type K, 4 – copper sleeve,  
5 – insulating cap, 6 – Teflon ring, 7 – heating surface

### 2.2. Data reduction and uncertainty estimation

The uncertainties of the measured and calculated parameters are estimated by mean-square method. Because heat flux density was calculated from the formula

$$q = \frac{UI}{\pi D_o L} = \frac{P}{\pi D_o L} \quad (1)$$

the experimental uncertainty of heat flux density was estimated as follows:

$$\Delta q = \sqrt{\left(\frac{\partial q}{\partial P} \Delta P\right)^2 + \left(\frac{\partial q}{\partial D_o} \Delta D_o\right)^2 + \left(\frac{\partial q}{\partial L} \Delta L\right)^2} \quad (2)$$

Where the absolute measurement errors of the electrical power  $\Delta P$ , outside tube diameter  $\Delta D_o$  and active length of a tube  $\Delta L$  are 10 W, 0.02 mm, and 0.2 mm, respectively. So, the maximum overall experimental limits of error for heat flux density extended from  $\pm 1.3\%$  for the maximum heat flux density up to  $\pm 1.2\%$  for the minimum heat flux density.

The average heat transfer coefficient was calculated as

$$\alpha = \frac{q}{\Delta T} = \frac{q}{(T_w - T_f)} \quad (3)$$

The experimental uncertainty for the average heat transfer coefficient is calculated as

$$\Delta \alpha = \sqrt{\left(\frac{\partial \alpha}{\partial q} \Delta q\right)^2 + \left(\frac{\partial \alpha}{\partial \Delta T} \delta T\right)^2} \quad (4)$$

where the absolute measurement error of the wall superheat,  $\delta T$ , estimated from the systematic error analysis equals  $\pm 0.2$  K. The maximum error for the average heat transfer coefficient was estimated to  $\pm 2.3\%$ .

### 2.3. Tested nanofluids

In the present study  $Al_2O_3$  and copper nanoparticles were used while distilled, deionised water was

applied as the base fluid. Nanofluids with different concentrations were prepared for the experiments. Nanoparticles of the required amount and the base liquid were mixed together. Ultrasonic vibration was used for 4 h in order to stabilise the dispersion of the nanoparticles. Alumina and copper nanoparticles were tested at the concentration of 0.01%, 0.1%, and 1% by weight. Alumina ( $\text{Al}_2\text{O}_3$ ) nanoparticles, of spherical form have a diameter from 5 nm to 250 nm; their mean diameter was estimated to be 47 nm according to the manufacturer (Sigma-Aldrich Co.). Copper nanoparticles, of a spherical form had a diameter from 7 nm to 257 nm; their mean diameter was estimated to be 48 nm according to the manufacturer (Sigma-Aldrich Co.). The photographs of the tested nanofluids are shown in Cieśliński and Kaczmarczyk (2011). The results of the thermal conductivity of the nanofluids measurements are discussed in Cieśliński and Kaczmarczyk (2011), as well.

### 3. RESULTS

Figure 3 and Fig. 4 show boiling curves for water- $\text{Al}_2\text{O}_3$  nanofluid of different concentrations (0.01%, 0.1% and 1%) boiling at subatmospheric pressure and overpressure, respectively. Generally, independent of operating pressure, sub- and atmospheric pressure, and overpressure, an increase of nanoparticle concentration augmented heat transfer.

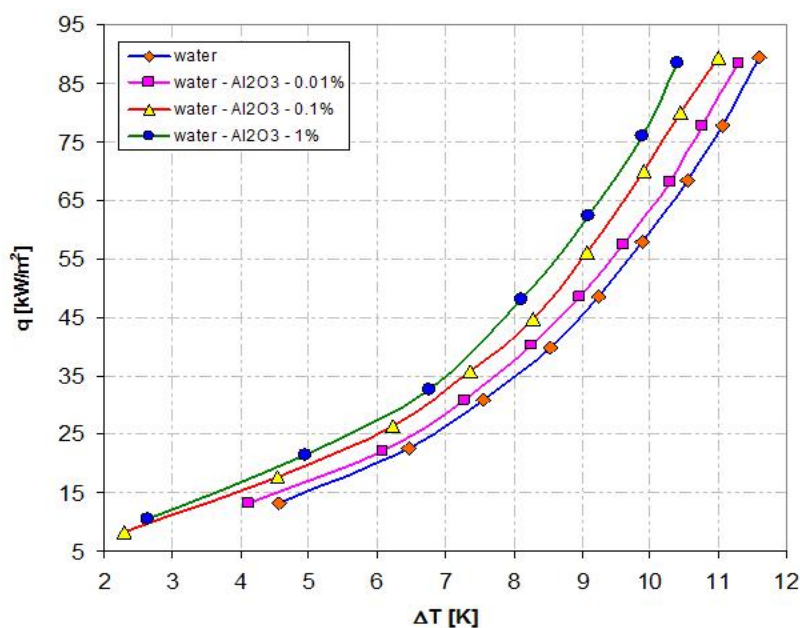


Fig. 3. Influence of concentration of water- $\text{Al}_2\text{O}_3$  nanofluid while boiling at 10 kPa

Figure 5 and Fig. 6 illustrate that the heat transfer coefficient against the heat flux density for water- $\text{Al}_2\text{O}_3$  and water-Cu nanofluids of the same nanoparticle concentrations equal to 1% by weight, respectively. At subatmospheric pressure a higher heat transfer coefficient was obtained for water-Cu nanofluid, while at overpressure for water- $\text{Al}_2\text{O}_3$  nanofluid. Generally, at subatmospheric pressure, independent of concentration a higher heat transfer coefficient was obtained for water-Cu nanofluid. For overpressure (200 kPa) – except 0.01% concentration, a higher heat transfer coefficient was obtained for water- $\text{Al}_2\text{O}_3$  nanofluid. For atmospheric pressure, independent of concentration, a higher heat transfer coefficient was obtained for water-Cu nanofluid while boiling on the horizontal smooth stainless steel tube – Fig. 7 and Fig. 8.



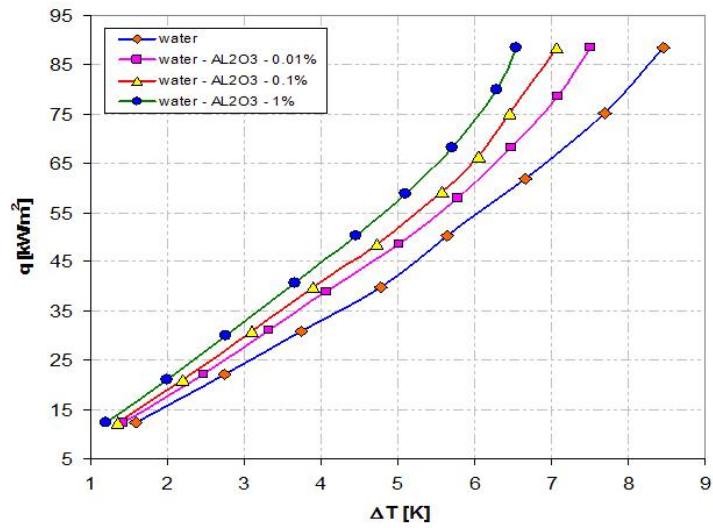


Fig. 4. Influence of concentration of water- $\text{Al}_2\text{O}_3$  nanofluid while boiling at 200 kPa

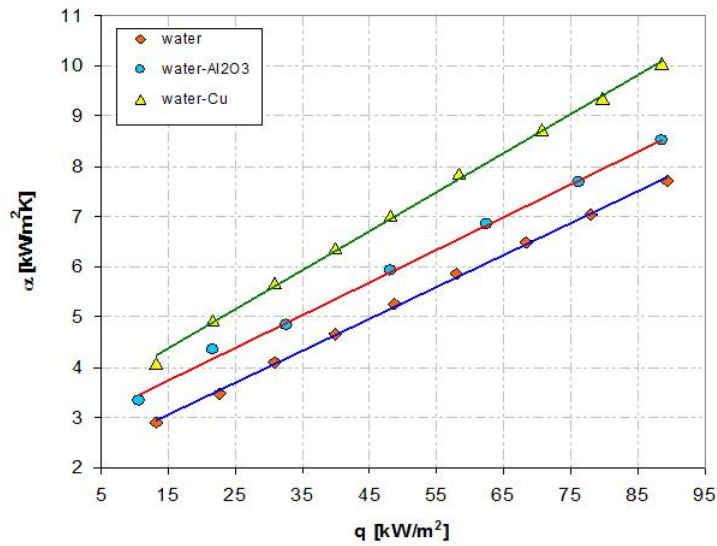


Fig. 5. Heat transfer coefficient vs. heat flux density for water- $\text{Al}_2\text{O}_3$  and water-Cu nanofluids of 1% concentration while boiling at 10 kPa

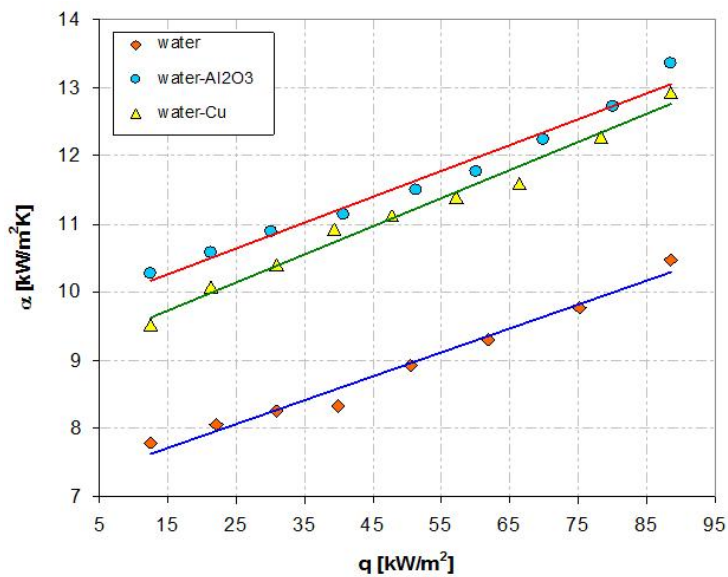


Fig. 6. Heat transfer coefficient vs. heat flux density for water- $\text{Al}_2\text{O}_3$  and water-Cu nanofluids of 1% concentration while boiling at 200 kPa

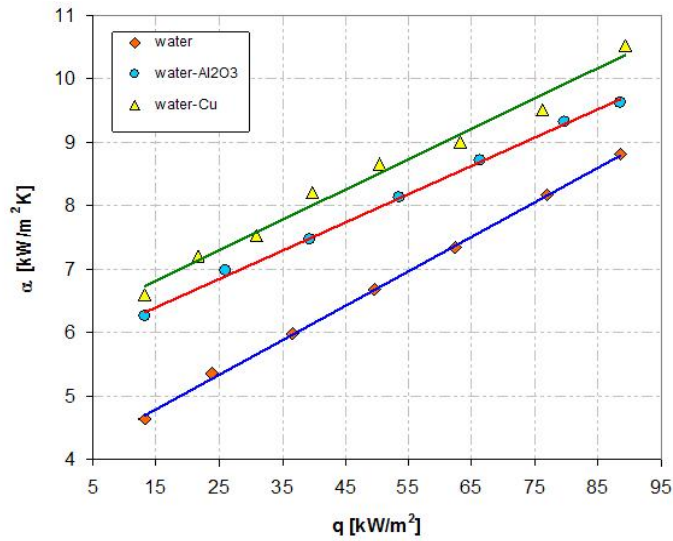


Fig. 7. Heat transfer coefficient vs. heat flux density for water- $\text{Al}_2\text{O}_3$  and water-Cu nanofluids of 0.01% concentration while boiling at atmospheric pressure

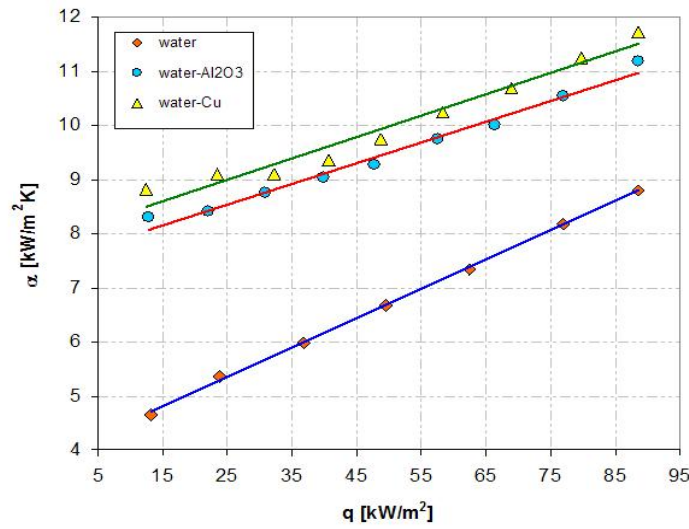


Fig. 8. Heat transfer coefficient vs. heat flux density for water- $\text{Al}_2\text{O}_3$  and water-Cu nanofluids of 1% concentration while boiling at atmospheric pressure

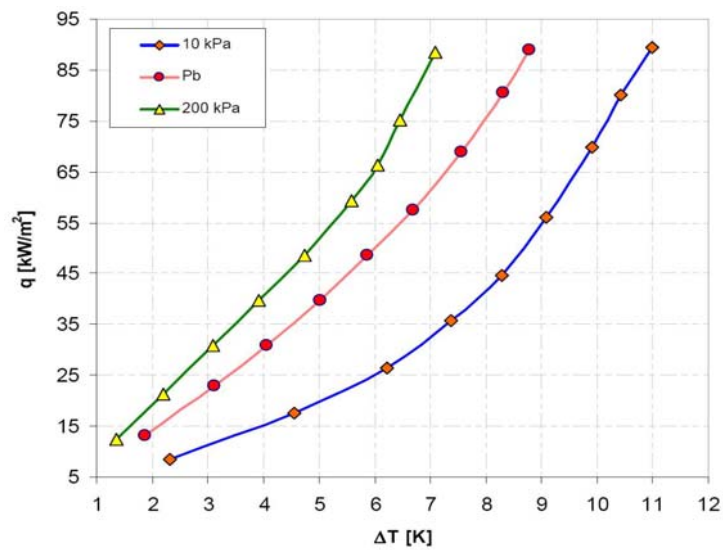


Fig. 9. Boiling curves of the smooth stainless steel tube in water- $\text{Al}_2\text{O}_3$  nanofluid with 0.1% concentration

Figure 9 and Fig. 10 display boiling curves for water-Al<sub>2</sub>O<sub>3</sub> and water-Cu nanofluids, respectively, with the same 0.1% concentration of nanoparticles, while boiling on the smooth stainless steel tube at different pressure.

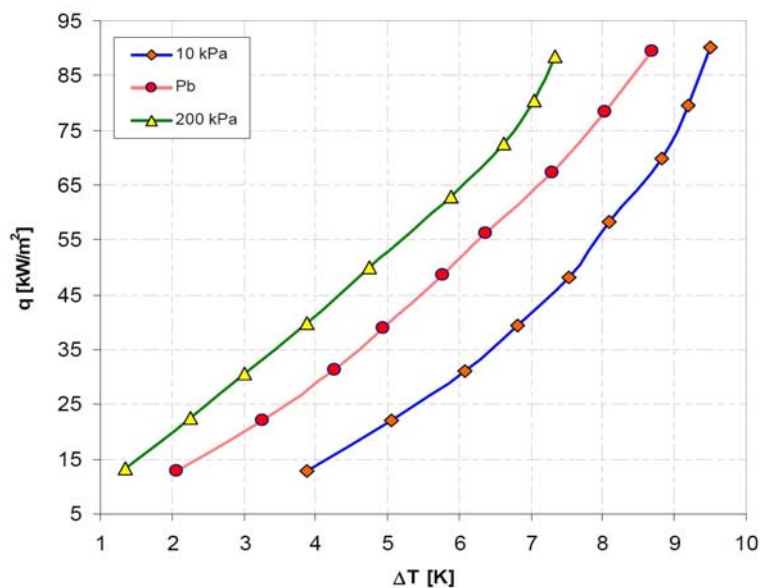


Fig. 10. Boiling curves of the smooth stainless steel tube in water-Cu nanofluid with 0.1% concentration

Independent of nanoparticle material (Al<sub>2</sub>O<sub>3</sub> and Cu) and concentration (0.01%, 0.1%, 1%) an increase of the operating pressure enhances heat transfer - boiling curves of the water-Al<sub>2</sub>O<sub>3</sub> and water-Cu nanofluids are shifted left, towards lower superheats. Nevertheless, as it is exemplified in Fig. 11 and Fig. 12, enhancement factor  $k_{eff}$  – defined as a ratio of the heat transfer coefficient for nanofluid to the heat transfer coefficient for distilled water at the same wall superheat, generally decreases with heat flux density increase. The exception is water-Cu nanofluid boiling at subatmospheric pressure, where - independent of concentration,  $k_{eff}$  increases with heat flux density increase.

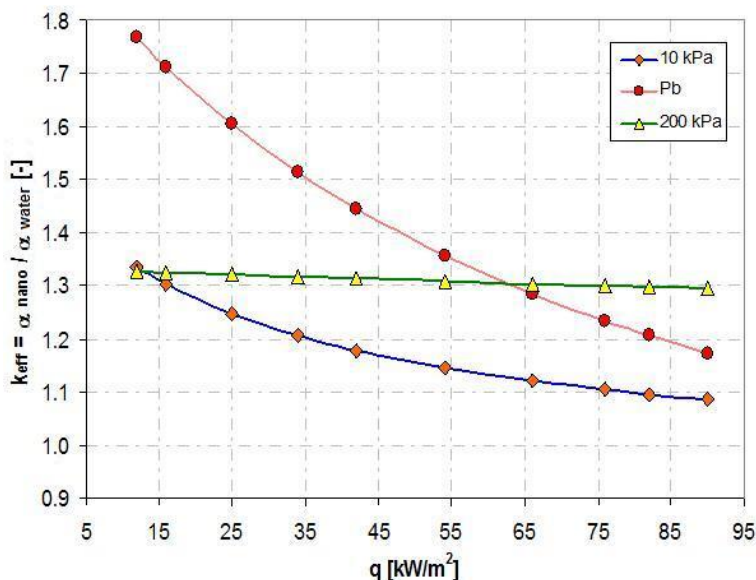


Fig. 11. Enhancement factor for water-Al<sub>2</sub>O<sub>3</sub> nanofluid of 0.1% nanoparticle concentration boiling on the smooth stainless steel tube

Figure 13 shows enhancement factors  $k_{eff}$  for both nanofluids tested of the same 1% nanoparticle concentration, i.e. water-Al<sub>2</sub>O<sub>3</sub> and water-Cu, while boiling on the smooth stainless steel tube at atmospheric pressure. As was mentioned above, generally, a higher heat transfer coefficient was



obtained for water-Cu nanofluid. Nevertheless, for both nanofluids tested the enhancement factor decreases distinctly with heat flux increase and the trends are similar.

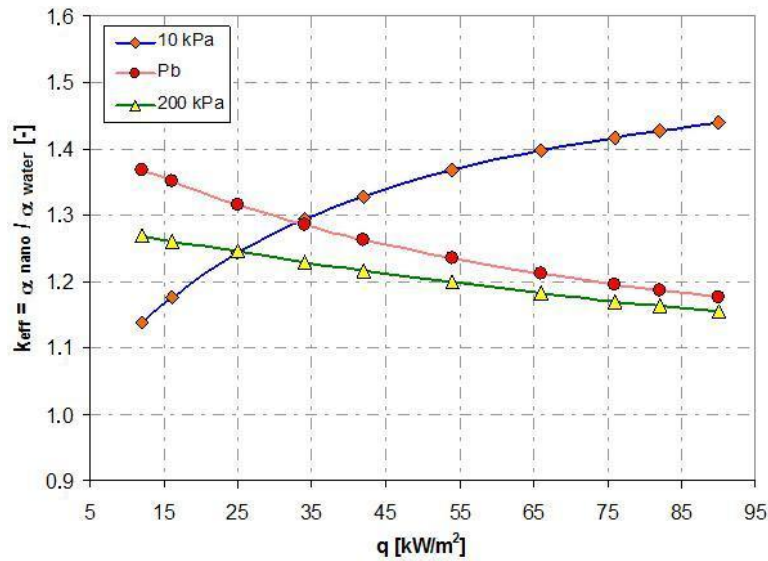


Fig. 12. Enhancement factor for water-Cu nanofluid of 0.1% nanoparticle concentration boiling on the smooth stainless steel tube

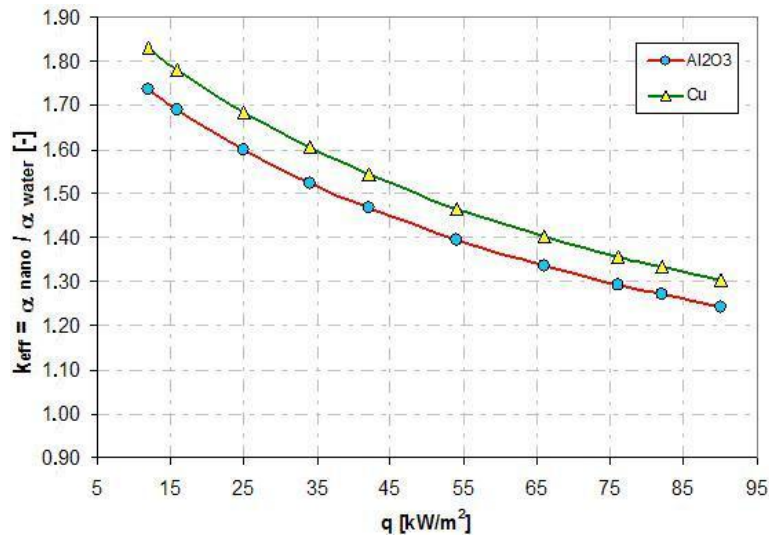


Fig. 13. Enhancement factor for water-Cu and water- $\text{Al}_2\text{O}_3$  nanofluids of 1% nanoparticle concentration while boiling on the smooth stainless steel tube

### 3.1. Discussion of the results

Having in mind the newest findings published in the literature as well as our own experience it seems that the decisive factor in heat transfer enhancement/deterioration mechanism during pool boiling of nanofluids is modification of the heating surface characteristics. There are several reasons of such a modification. First, because of nanoparticle agglomeration, even in the presence of surfactant/dispersant, nanofluids are unstable and agglomerates, due to sedimentation, are deposited on the heating surface. When the size of the particles and the size of the surface roughness are comparable, the particles settle in the voids of the surface and block nucleation sites which leads to heat transfer deterioration. When the particles are either much larger or much smaller than the size of heater surface roughness heat transfer enhancement is observed (Das et al., 2008). In the case of unstable suspension

of a very high nanoparticle concentration, agglomerates can create a nanoparticle coating generating an extra thermal resistance to the boiling surface and hence deteriorating heat transfer performance. Second, even if very stable nanofluids were used (the stability of the nanofluids can be augmented using electrostatic stabilisation) a nanoparticle coating was observed on the heater surface after the tests. As follows from Ahmed and Hamed (2010) and Kwark et al. (2010) studies, boiling itself appears to be responsible for nanoparticle coating formation and the primary mechanism of nanocoating creation is micro-layer evaporation during bubble growth.

The mechanistic models of nucleate boiling (Judd and Hwang, 1976; Benjamin and Balakrishnan, 1996) assume the additive mechanism of heat transfer comprising transient heat conduction, microlayer evaporation and turbulent natural convection in the area outside the influence of the bubbles. Each mentioned mode of heat transfer is affected by thermal conductivity of the boiling liquid, so the enhanced thermal conductivity of the nanofluids becomes a significant effect that augments the heat transfer performance.

Boiling is a process depending on the interaction between boiling liquid and heating surface, i.e. wettability (Wang and Dhir, 1993). As nanofluids exhibit improved wettability (Kim et al., 2007; Coursey and Kim, 2008) this is another factor augmenting boiling heat transfer.

#### 4. CONCLUSIONS

- An increase of nanoparticle concentration (0.01%, 0.1%, 1%) augmented heat transfer for the tested operating pressures (10 kPa, atmospheric pressure and 200 kPa).
- Independent of nanoparticle material ( $\text{Al}_2\text{O}_3$  and Cu) and its concentration an increase of operating pressure enhances heat transfer during boiling of water- $\text{Al}_2\text{O}_3$  and water-Cu nanofluids.
- Generally, independent of operating pressure, except one case - overpressure (200 kPa) and 0.01% nanoparticle concentration, a higher heat transfer coefficient was obtained for water-Cu nanofluid while boiling on the horizontal smooth stainless steel tube.
- Except for water-Cu nanofluid enhancement factor  $k_{\text{eff}}$  – defined as a ratio of the boiling heat transfer coefficient for nanofluid to the boiling heat transfer coefficient for distilled water at the same wall superheat, decreases with heat flux density increase.

*This work was sponsored by the Ministry of Research and Higher Education, Grant No. N N512 374435.*

#### SYMBOLS

$D$	outside tube diameter, m
$L$	active length of a tube, m
$P$	electrical power, W
$T$	temperature, K
$q$	heat flux density, $\text{W}/\text{m}^2$

#### *Greek symbols*

$\alpha$	average heat transfer coefficient, $\text{W}/(\text{m}^2\text{K})$
----------	--

#### *Subscripts*

$w$	<i>wall</i>
-----	-------------

*f* fluid

## REFERENCES

- Ahmed O., Hamed M.S., 2010. The effect of experimental techniques on the pool boiling of nanofluids. *Proc. 7<sup>th</sup> Int. Conf. on Multiphase Flow, ICMF 2010*, Tampa, FL USA, May 30-June 4.
- Bang I. C., Chang S. H., 2005. Boiling heat transfer performance and phenomena of  $\text{Al}_2\text{O}_3$  – water nano-fluids from a plain surface in a pool. *Int. J. Heat Mass Transf.*, 48, 2407-2419. DOI: 10.1016/j.ijheatmasstransfer.2004.12.047.
- Benjamin R.J., Balakrishnan A.R., 1997. Nucleation site density in pool boiling of saturated pure liquids: effect of surface microroughness and surface and liquid physical properties. *Exp. Thermal Fluid Sci.*, 15, 32-42. DOI: 10.1016/S0894-1777(96)00168-9.
- Bergles A.E., 1985. *Techniques to augment heat transfer. Handbook of heat transfer applications*. New York, McGraw-Hill, 3-1-80.
- Bi S., Guo K., Liu Z., Wu J., 2011. Performance of a domestic refrigerator using  $\text{TiO}_2$ -R600a nano-refrigerant as working fluid. *Energy Conversion and Management*, 52, 733–737. DOI: 10.1016/j.enconman.2010.07.052.
- Choi S., 1995. Enhancing thermal conductivity of fluids with nanoparticles, In: Siginer D.A., Wang H.P. (Eds.), *Developments and Applications of Non-Newtonian Flows*, ASME, FED-Vol. 231/MD-Vol. 66, 99-105.
- Cieśliński J.T., Krasowski K., Kaczmarczyk T., 2007. Simulation of temperature field in cylindrical boiling heating section. *Turbulence: Int. J.*, 12, 59 – 64.
- Cieśliński J.T., Kaczmarczyk T.Z., 2011. Pool boiling of water- $\text{Al}_2\text{O}_3$  and water-Cu nanofluids on horizontal smooth tubes. *Nanoscale Research Letters*, 6, 220. DOI:10.1186/1556-276X-6-220.
- Cieśliński J.T., Rubalewski J., 2012. Effect of nanofluid concentration on two-phase thermosyphon heat exchanger performance. *International Symposium on Multiphase Flow and Transport Phenomena*. April 22-25, 2012, Agadir, Morocco.
- Coursey J. S., Kim J., 2008. Nanofluid boiling: The effect of surface wettability, *Int. J. Heat Fluid Flow*, 29, 1577-1585. DOI: 10.1016/j.ijheatfluidflow.2008.07.004.
- Das S. K., Putra N., Roetzel W., 2003. Pool boiling characteristics of nano-fluids. *Int. J. Heat Mass Transf.*, 46, 851-862. DOI: 10.1016/S0017-9310(02)00348-4.
- Das S.K., Narayan G.P., Baby A.K., 2008. Survey on nucleate pool boiling of nanofluids: the effect of particle size relative to roughness. *J. Nanopart. Res.*, 10, 1099-108. DOI: 10.1007/s11051-007-9348-x.
- Hadad K., Hajizadeh A., Jafarpour K., Ganapol B.D., 2010. Neutronic study of nanofluids application to VVER-1000. *Annals of Nuclear Energy*, 37, 1447–1455. DOI: 10.1016/j.anucene.2010.06.020.
- Judd R.L., Hwang K.S., 1976. A comprehensive model for nucleate pool boiling heat transfer including microlayer evaporation. *ASME J. Heat Transf.*, 98, 623-629.
- Kang S.W., Wei W.C., Tsai S.H., Shih-Yu Yang S.Y., 2006. Experimental investigation of silver nano-fluid on heat pipe thermal performance. *Appl. Thermal Eng.*, 26, 2377–2382. DOI: 10.1016/j.applthermaleng.2006.02.020.
- Kashinath M. R., 2006. *Parameters affecting critical heat flux of nanofluids: heater size, pressure, orientation and anti-freeze addition*, MSc Thesis, The University of Texas at Arlington.
- Kathiravan R., Kumar R., Gupta A., Chandra R., 2010. Preparation and pool boiling characteristics of copper nanofluids over a flat plate heater. *Int. J. Heat Mass Transf.*, 53, 1673-1681. DOI: 10.1016/j.ijheatmasstransfer.2010.01.022.
- Kim S.J., Bang I.C., Buongiorno J., Hu L.W., 2007. Surface wettability change during pool boiling of nanofluids and its effect on critical heat flux. *Int. J. Heat Mass Transfer*, 50, 4105-4116. DOI: 10.1016/j.ijheatmasstransfer.2007.02.002.
- Kim S.J., McKrell T., Buongiorno J., Hu L.W., 2010. Subcooled flow boiling heat transfer of dilute alumina, zinc oxide, and diamond nanofluids at atmospheric pressure. *Nuclear Eng.Des.*, 240, 1186–1194. DOI: 10.1016/j.nucengdes.2010.01.020.
- Kleinstreuer C., 2011. Experimental and theoretical studies of nanofluid thermal conductivity enhancement: A review, *Nanoscale Res. Lett.*, 6, 229. DOI:10.1186/1556-276X-6-229.
- Kwark S.M., Kumar R., Moreno G., Yoo J., You S. M., 2010. Pool boiling characteristics of low concentration nanofluids, *Int. J. Heat Mass Transfer*, 53, 972-981. DOI: 10.1016/j.ijheatmasstransfer.2009.11.018.

- Leong K.Y., Saidur R., Kazi S.N., Mamun A.H., 2010. Performance investigation of an automotive car radiator operated with nanofluid-based coolants (nanofluid as a coolant in a radiator). *Applied Thermal Engineering*, 30, 2685-2692. DOI: 10.1016/j.applthermaleng.2010.07.019.
- Li C.H., Wang B.X., Peng X. F., 2003. Experimental investigations on boiling of nano-particle suspensions. *5<sup>th</sup> Int. Conf. Boiling Heat Transfer*. Montego Bay, Jamaica, 4-8 July 2003.
- Liu Z. -H., Yang X. -F., Xiong J. -G., 2010. Boiling characteristics of carbon nanotube suspensions under sub-atmospheric pressures. *Int. J. Thermal Sci.*, 49, 1156-1164. DOI: 10.1016/j.ijthermalsci.2010.01.023.
- Liu Z., Liao L., 2008. Sorption and agglutination phenomenon of nanofluids on a plain heating surface during pool boiling. *Int. J. Heat Mass Transf.*, 51, 2593-2602. DOI: 10.1016/j.ijheatmasstransfer.2006.11.050
- Liu Z., Xiong J., Bao R., 2007. Boiling heat transfer characteristics of nanofluids in a flat heat pipe evaporator with micro-grooved heating surface. *Int. J. Multiphase Flow*, 33, 1284-1295. DOI: 10.1016/j.ijmultiphaseflow.2007.06.009.
- Lotfi H., Shafii M.B., 2009. Boiling heat transfer on a high temperature silver sphere in nanofluid. *Int. J. Thermal Sci.*, 48, 2215-2220. DOI: 10.1016/j.ijthermalsci.2009.04.009.
- Marto P. J., Anderson C. L., 1992. Nucleate boiling characteristics of R-113 in small tube bundle. *Transactions ASME J. Heat Transf.*, 114, 425-433.
- Narayan G. P., Anoop K. B., Sateesh G., Das S. K., 2008. Effect of surface orientation on pool boiling heat transfer of nanoparticle suspensions. *Int. J. Multiphase Flow*, 34, 145-160. DOI: 10.1016/j.ijmultiphaseflow.2007.08.004.
- Shi M. H., Shuai M. Q., Lai Y. E., Li Y. Q., Xuan M., 2006. Experimental study of pool boiling heat transfer for nanoparticle suspensions on a plate surface. *13<sup>th</sup> Int. Heat Transfer Conference*, Sydney, Australia, 13-18 August, paper BOI-06.
- Trisaksri V., Wongwises S., 2009. Nucleate pool boiling heat transfer of TiO<sub>2</sub>-R141b nanofluids. *Int. J. Heat Mass Transf.*, 52, 1582-1588. DOI: 10.1016/j.ijheatmasstransfer.2008.07.041.
- Vassallo P., Kumar R., Amico S., 2004. Pool boiling heat transfer experiments in silica-water nano-fluids. *Int. J. Heat Mass Transf.*, 47, 407-411. DOI: 10.1016/S0017-9310(03)00361-2.
- Wang C.H., Dhir V.K., 1993. Effect of surface wettability on active nucleation site density during pool boiling of saturated water. *ASME. J. Heat Transf.*, 115, 659-669.
- Wen D., Ding Y., 2005. Experimental investigation into the boiling heat transfer of aqueous based  $\gamma$ -alumina nanofluids. *J. Nanopart. Res.*, 7, 265-274. DOI: 10.1007/s11051-005-3478-9.
- Yang X.F., Liu Z.H., 2011. Application of functionalized nanofluid in thermosyphon. *Nanoscale Res. Lett.*, 6, 494. DOI:10.1186/1556-276X-6-494.
- You S. M., Kim J. H., Kim K. H., 2003. Effect of nanoparticles on critical heat flux of water in pool boiling heat transfer. *Appl. Physics Lett.*, 83, 3374-3376. DOI: 10.1063/1.1619206.

Received 17 August 2011

Received in revised form 15 December 2011

Accepted 15 December 2011